

CRYSTALLIZATION P 132-135

Crystallization and preliminary crystallographic analysis of a zinc-dependent alcohol dehydrogenase from *Streptococcus pneumoniae*

Donghyuk Shin and Sangho Lee*

Department of Biological Sciences, Sungkyunkwan University, 2066 Seobu-ro, Suwon 16419, Republic of Korea

*Correspondence: sangholee@skku.edu

Alcohol dehydrogenase (ADH) is one of essential enzymes for all living organisms, and conserved from archaea to mammals. The most abundant type of ADH is zinc-containing one. All the zinc containing ADHs possess the catalytic zinc site, while some have the second, structural zinc site. ADHs require either NAD(H) or NADP(H) as a cofactor. Despite lots of efforts to determine the key residues for cofactor specificity of ADHs, there is no general rule for cofactor specificity so far. To establish the general rules for the cofactor specificity of ADHs by structural analysis, we cloned and overexpressed the zinc dependent alcohol dehydrogenase from *Streptococcus pneumoniae* strain D39 (SpADH2) in *Escherichia coli*. Rod-shape crystals of SpADH2 were obtained by hanging-drop vapour diffusion from a reservoir solution containing 50 mM Tris-HCl pH 8.0, 50 mM NaCl, PEG 3350 15% (w/v) and diffracted to 2.19 Å resolution. Crystal belonged to orthorhombic space group $P2_12_12_1$, with unit cell parameters $a = 88.2$ Å, $b = 123.2$ Å, $c = 130.4$ Å and contained four molecules in the asymmetric unit.

INTRODUCTION

Cofactor specificity toward NADP(H) or NAD(H) of dehydrogenase enzyme families are extensively studied for decades. The cofactor specificity of *Corynebacterium* 2,5-diketo-D-gluconic acid (2,5-DKG) reductase was successfully converted from NADPH to NADH (Banta et al., 2002a, b). Complete reversal of cofactor specificity from NADPH to NADH was also achieved by engineering the phosphate binding pocket of an alcohol dehydrogenase (ADH8) from *Rana perezi* (Rosell et al., 2003). For *myo*-inositol dehydrogenase (IDH) from *Bacillus subtilis*, the cofactor specificity is changed from NAD to NADP, and twisted nicotinamide group of NADP was observed in the binding pocket from crystal structure (Zheng et al., 2013). Conversion of the cofactor specificity from NADPH to NADH in an alcohol dehydrogenase from *Escherichia coli* (AdhZ3) has been extensively documented. By a computational method with structure-guided site-specific random mutagenesis, AdhZ3 was revealed to utilize NADH as its cofactor (Pick et al., 2014). Crystal structures of homoserine dehydrogenase (HseDH) from *Pyrococcus horikoshii* revealed that HseDH can bind both NADPH and NADH. In this case, NADPH acts as a strong inhibitor of NAD, rather than as a cofactor (Hayashi et al., 2015). Recently, a thermostable alcohol dehydrogenase (AdhD) from *Pyrococcus furiosus* suggests that loop insertion after the cofactor binding pockets may alter the cofactor specificity (Solanki et al., 2017). While there were lots of efforts to determine the key residues for the cofactor specificity of ADHs, there is no general

rule so far. The most abundant type of ADH is zinc-containing one. All the zinc containing ADHs possess the catalytic zinc site, while some have the second, structural zinc site. To expand our knowledge and to establish general rules for cofactor specificity of ADHs by structural analysis, we cloned, overexpressed and crystallized a zinc-dependent alcohol dehydrogenase (ADH2) from *Streptococcus pneumoniae* (SpADH2).

RESULTS AND DISCUSSION

The GST tagged SpADH2 (GST-SpADH2) was expressed in *E. coli* and purified by affinity chromatography. The GST-SpADH2 was cleaved by the GFP-TEV protease, and further purified by size exclusion chromatography. Purification steps of the GFP-TEV protease treatment were monitored by SDS-PAGE (Figure 1a). Purified SpADH2 was concentrated to 8 mg ml⁻¹, and subjected to dynamic light scattering to check the polydispersity. SpADH2 was monodisperse in solution judged by dynamic light scattering (Figure 1b). Initial crystals with overlapped rod shape were obtained from reservoir solutions containing PEG 4000 as a precipitant. After refining the initial crystallization conditions, single rod-shape crystals were obtained in reservoir solutions containing PEG 3350 as a precipitant instead of PEG 4000 (Figure 2). The best SpADH2 crystal diffracted up to 2.19 Å resolution (Figure 3). Initial data reduction revealed that the SpADH2 crystal belonged to the space group $P2_12_12_1$, with unit cell parameters $a = 88.177$ Å, $b = 123.245$ Å and $c = 130.356$ Å. Data collection and

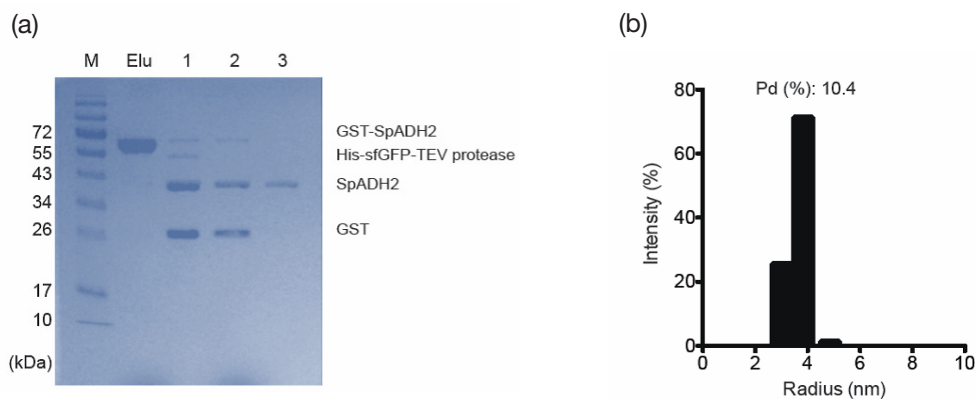


FIGURE 1 | Purification of SpADH2. (a) (Lane Elu) GST-SpADH2 was purified with affinity chromatography (Glutathione 4B sepharose, GE Healthcare Life Sciences), and (Lane 1) His-tagged super-fold GFP-TEV (His-sfGFP-TEV) protease was added to cleave the N-terminal GST tag of SpADH2. (Lanes 2 and 3) The samples after cleavage by the sfGFP-TEV protease were loaded onto Ni-NTA and glutathione-Sepharose beads to capture His-sfGFP-TEV protease and the cleaved GST protein or the uncleaved GST-SpADH2. (b) Polydispersity (Pd) of SpADH2 was measured by dynamic light scattering (DLS). Regularization histogram indicates that purified SpADH2 proteins are monodisperse in solution.

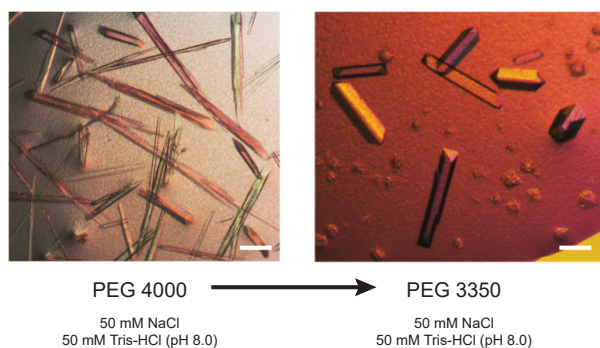


FIGURE 2 | Crystallization of SpADH2.

(Left) Initial crystals of SpADH2 were obtained in overlapped rod shape after 2 days from a reservoir solution containing 50 mM NaCl, 50 mM Tris-HCl pH 8.0, and 15% (w/v) PEG 4000. (Right) Single rod shape crystals could be obtained from a reservoir solution containing 50 mM NaCl, 50 mM Tris-HCl pH 8.0, and 15% (w/v) PEG 3350. Scale-bar, 100 μ m.

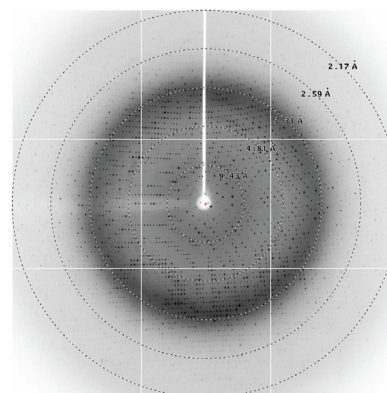


FIGURE 3 | A representative 1° oscillation X-ray diffraction image from the SpADH2 crystal. The diffraction limits are indicated with circles.

TABLE 1 | Macromolecule-production information

Source organism	<i>Streptococcus pneumoniae</i> strain D39
DNA source	Genomic DNA
Forward primer	<i>Bam</i> HI CCG GGA TCC ATG AAA GCC TAT ACT TAT GTT AAA CC
Reverse primer	<i>Xho</i> I CCG CTC GAG TTA GGC TTC TGA GAT ATC GTT TTC
Cloning vector	Parallel GST2
Expression vector	Parallel GST2
Expression host	<i>Escherichia coli</i> strain BL21(DE3)
Complete amino acid sequence of the construct produced	MKAYTYVKPLGASFVDVDPKPIVRKPTDAIVRIVKTTICGTDLHIIKGDVPTCQSGTILGHEGIGIVEEVGEG VSNFKKGDKVLISCVACGCKCYCKKGIYAHCEDEGGWIFGHLIDGMQAEYLRVPHADNTLYHTPED LSDEALVMLS DILPTGYEIGVLKGVKVEPGCSVAIIGSGPVGLAALLTAQFYS PAKLIMVDLDDNRLETALS FGATHKVNSSDPEKAIKEIYDLTDGRGVDVAIEAVGIPATFDQCQKIIGVDGTVANCGVHGKPVVEFDLTKL WIRNINVTTGLVSTNTTPQLLKALESHKIEPEKLVTHYFKLSEIEKAYEVFSKAADHHAIKVIENDISEA

TABLE 2 | Crystallization

Method	Hanging drop vapor diffusion
Plate type	24-well plate
Temperature (K)	295
Protein concentration	8 mg ml ⁻¹
Buffer composition of protein solution	50 mM Tris-HCl pH 7.5 and 20 mM NaCl
Composition of reservoir solution	50 mM Tris-HCl pH 8.0, 50 mM NaCl, and PEG 3350 15% (w/v)
Volume and ratio of drop	2 μ l protein solution with 2 μ l reservoir solution
Volume of reservoir	500 μ l

TABLE 3 | Data collection and processing statistics

Crystal	SpADH2
Diffraction source	PAL 5C
Wavelength (Å)	1.28277
Temperature (K)	100
Detector	ADSC Quantum 315R
Rotation range per image (°)	1
Exposure time per image (s)	1
Space group	<i>P</i> 2 ₁ 2 ₁ 2 ₁
<i>a</i> , <i>b</i> , <i>c</i> (Å)	88.177, 123.245, 130.356
α , β , γ (°)	90, 90, 90
Resolution range (Å)	41.51 – 2.189 (2.267 – 2.189)*
Total No. of reflections	847394 (85636)
No. of unique reflections	73418 (7178)
Completeness (%)	99.0 (98.0)
Redundancy	14.4 (14.6)
$\langle I/\sigma(I) \rangle$	33.73 (7.03)
R_{merge}	0.093(0.598)
R_{meas}	0.098 (0.624)
Overall <i>B</i> factor from Wilson plot (Å ²)	37.84

* Values for the outer shell are given in parentheses.

processing statistics are summarized in Table 3. Based on the Matthews coefficient (V_M) being 2.24 Å³ Da⁻¹ and a solvent content of 45.0% (Matthews, 1968), the asymmetric unit seems to contain two dimers (four molecules) of SpADH2. Phases of SpADH2 were determined by molecular replacement using EhADH (PDB ID: 2NVB) (Goinberg et al., 2008) as a template showing 30% sequence identity. Phasing by molecular replacement and preliminary structure refinement is currently under way using PHENIX (Adams et al., 2010).

METHODS

Protein expression and purification

Gene encoding *adh2* from *Streptococcus pneumoniae* strain D39 (GenBank

accession number: NC_008533.1) was amplified and inserted into parallel GST2 vector (Sheffield et al., 1999) using restriction enzymes *Bam*HI and *Xho*I to produce GST-tagged SpADH2. The pGST2-SpADH2 plasmid was transformed into *Escherichia coli* BL21(DE3) strain (Table 1). Cell were incubated at 310K in LB medium supplemented with 50 μ g ml⁻¹ ampicillin and 1 mM zinc chloride, grown to OD₆₀₀ of 0.6-0.8, then induced with 0.5 mM isopropyl-1-thio- β -D-galactopyranoside at 293K. The induced cells were further grown for 20 h at 293K. Following harvesting cells by centrifugation at 4,000 rpm for 15 min at 277 K, the cells were suspended in buffer A (50 mM Tris-HCl pH 7.5 and 150 mM NaCl), then lysed by sonication. Supernatant containing soluble GST-SpADH2 was collected by centrifugation at 13,000 rpm for 1h at 277K and loaded onto glutathione-4B-Sepharose beads (GE HealthCare). After incubating and washing with buffer B (50 mM Tris-HCl pH 7.5 and 0.5 M NaCl), the protein was eluted in buffer C (50 mM Tris-HCl pH 8.0, 50 mM NaCl and 15 mM reduced glutathione). GST-tag was cleaved by super-fold GFP-tagged tobacco etch virus (sfGFP-TEV) protease (Wu et al., 2009) during dialysis against buffer D (25 mM Tris-HCl pH 7.5, 75 mM NaCl, and 0.5 mM EDTA) overnight at 277K, and the resulting solution was supplemented with 10 mM imidazole and loaded to Ni-NTA agarose and glutathione-4B-sepharose beads to remove the tobacco etch virus protease and the cleaved GST-tag, respectively. Flow-through was collected and further purified on a HiTrap Q ion-exchange column (GE HealthCare) in buffer E (20 mM Tris-HCl pH 7.5 with a linear gradient of 10 mM – 500 mM NaCl) and subsequently on a HiLoad 16/600 Superdex-200 prep-grade size exclusion column (GE HealthCare) pre-equilibrated with buffer F (50 mM Tris-HCl pH 7.5 and 20 mM NaCl). SpADH2 was concentrated up to 8 mg ml⁻¹ using a 10 kDa-centrifugal filter (Ambicom Ultra). The protein concentrations were determined by measuring absorbance at 280 nm.

Crystallization

Prior to crystallization, polydispersity of the concentrated SpADH2 was checked by dynamic light scattering on a DynaPro 100 system (Wyatt Technology). Crystallization was carried out at 295K with 8 mg ml⁻¹ protein by hanging-drop vapour diffusion method. Initial crystallization screening was performed using commercial screening kits using Crystal Screen (Hampton Research) and Wizard Screen (Emerald Bioscience). Diffraction-quality crystal of SpADH2 was obtained by mixing 2 μ l protein solution with 2 μ l reservoir solution containing 50 mM Tris-HCl pH 8.0, 50 mM NaCl and PEG 3350 15% (w/v) at 295K (Table 2).

Data collection and processing

SpADH2 native crystals were transferred to a cryoprotectant solution with 30% glycerol supplemented to the reservoir condition. Diffraction data was collected on single frozen crystal in a gaseous nitrogen stream at 100K over a range 360° with a rotation angle per image of 1.0° at beamline 5C at Pohang Accelerator Laboratory (Park et al., 2007). The native SpADH2 crystal diffracted to maximum resolution of 2.19 Å. Data processing and reduction were carried out using *HKL-2000* (Otwinowski and Minor, 1997). The data collection and processing statistics are summarized in Table 3.

CONFLICT OF INTEREST

The authors declare no conflict of interest.

ACKNOWLEDGEMENTS

We thank the staff members at Pohang Accelerator Laboratory beamlines 5C for data collection and Professor Dong-Kwon Rhee at Sungkyunkwan University for providing genomic DNA. This work was supported by the Basic Science Research Program (NRF-2017R1D1A1B03032185) and the Science Research Center Program (SRC-2017R1A5A1014560) through the National Research Foundation of Korea (NRF).

Original Submission: Nov 30, 2017

Revised Version Received: Dec 18, 2017

Accepted: Dec 18, 2017

REFERENCES

- Adams, P.D., Afonine, P.V., Bunkoczi, G., Chen, V.B., Davis, I.W., Echols, N., Headd, J.J., Hung, L.W., Kapral, G.J., Grosse-Kunstleve, R.W., McCoy, A.J., Moriarty, N.W., Oeffner, R., Read, R.J., Richardson, D.C., et al. (2010). PHENIX: a comprehensive Python-based system for macromolecular structure solution. *Acta Crystallogr D Biol Crystallogr* **66**, 213-221.
- Banta, S., Swanson, B.A., Wu, S., Jarnagin, A., and Anderson, S. (2002a). Alteration of the specificity of the cofactor-binding pocket of *Corynebacterium* 2,5-diketo-D-gluconic acid reductase A. *Protein Eng* **15**, 131-140.
- Banta, S., Swanson, B.A., Wu, S., Jarnagin, A., and Anderson, S. (2002b). Optimizing an artificial metabolic pathway: engineering the cofactor specificity of *Corynebacterium* 2,5-diketo-D-gluconic acid reductase for use in vitamin C biosynthesis. *Biochemistry* **41**, 6226-6236.
- Goihberg, E., Dym, O., Tel-Or, S., Shimon, L., Frolow, F., Peretz, M., and Burstein, Y. (2008). Thermal stabilization of the protozoan *Entamoeba histolytica* alcohol dehydrogenase by a single proline substitution. *Proteins* **72**, 711-719.
- Hayashi, J., Inoue, S., Kim, K., Yoneda, K., Kawarabayasi, Y., Ohshima, T., and Sakuraba, H. (2015). Crystal Structures of a Hyperthermophilic Archaeal Homoserine Dehydrogenase Suggest a Novel Cofactor Binding Mode for Oxidoreductases. *Sci Rep* **5**, 11674.
- Matthews, B.W. (1968). Solvent content of protein crystals. *J Mol Biol* **33**, 491-497.
- Otwinowski, Z., and Minor, W. (1997). Processing of X-ray diffraction data collected in oscillation mode. *Methods Enzymol* **276**, 307-326.
- Park, S.-Y., Ha, S.-C., and Kim, Y.-G. (2007). The Protein Crystallographic Beamlines at the Pohang Light Source II. *Biodesign* **5**, 30-34.
- Pick, A., Ott, W., Howe, T., Schmid, J., and Sieber, V. (2014). Improving the NADH-cofactor specificity of the highly active AdhZ3 and AdhZ2 from *Escherichia coli* K-12. *J Biotechnol* **189**, 157-165.
- Rosell, A., Valencia, E., Ochoa, W.F., Fita, I., Pares, X., and Farres, J. (2003). Complete reversal of coenzyme specificity by concerted mutation of three consecutive residues in alcohol dehydrogenase. *J Biol Chem* **278**, 40573-40580.
- Sheffield, P., Garrard, S., and Derewenda, Z. (1999). Overcoming expression and purification problems of RhoGDI using a family of "parallel" expression vectors. *Protein Expr Purif* **15**, 34-39.
- Solanki, K., Abdallah, W., and Banta, S. (2017). Engineering the cofactor specificity of an alcohol dehydrogenase via single mutations or insertions distal to the 2'-phosphate group of NADP(H). *Protein Eng Des Sel* **30**, 373-380.
- Wu, X., Wu, D., Lu, Z., Chen, W., Hu, X., and Ding, Y. (2009). A novel method for high-level production of TEV protease by superfolder GFP tag. *J Biomed Biotechnol* **2009**, 591923.
- Zheng, H., Bertwistle, D., Sanders, D.A., and Palmer, D.R. (2013). Converting NAD-specific inositol dehydrogenase to an efficient NADP-selective catalyst, with a surprising twist. *Biochemistry* **52**, 5876-5883.